PERGAMON

Energy Conversion and Management 44 (2003) 961–973

ENERGY CONVERSION & MANAGEMENT

www.elsevier.com/locate/enconman

# Second law analysis of thermodynamics in the electric arc furnace at a steel producing company

Ünal Çamdali [a,*], Murat Tunç [b], Ahmet Karakaş [b]

[a] *Development Bank of Turkey, Necatibey Cad., No: 98, Bakanliklar, 06100 Ankara, Turkey*
[b] *Department of Mechanical Engineering, Istanbul Technical University, Gumussuyu, 80191 Istanbul, Turkey*

Received 15 October 2001; accepted 20 March 2002

**Abstract**

In this study, energy and conservation analyses are applied to the production of steel process in the electric arc furnace. The scrap pre-heating system, stack gas and cooling water leaving the furnace are investigated, and the obtained results are compared with experimental ones.


*Keywords:* Second law analysis; Electric arc furnace; Thermodynamic and heat analyses

## 1. Introduction

Industrial energy processes can be analyzed through economic assessment of the losses associated with the production phases. In recent years, several authors have undertaken energy analyses of efficient use of energy in different phases of industrial processes [1,2].

The fact that approximately 12 percent of the world energy production is used in the iron and steel industry justifies very much the use of energy saving methods in the industry. Today, application of the second law of thermodynamics is generally preferred in energy analysis, since it gives more correct, reliable and meaningful results.

* Corresponding author.
*E-mail addresses:* ucamdali@ttnet.net.tr, ucamdali@yahoo.com (Ü. Çamdali), tuncmu@itu.edu.tr (M. Tunç).

0196-8904/02/$ - see front matter 
PII: S0196-8904(02)00086-9

**Nomenclature**

| | |
|---|---|
| $A$ | area ($m^2$) |
| $c_p$, $\bar{c}_p$ | constant pressure specific heat (kJ/kg K; kJ/kmol K; kcal/kmol K) |
| $D$ | diameter (m) |
| EAF | electric arc furnace |
| $Gr$ | Grashof number |
| $h$ | heat transfer coefficient (kJ/$m^2$ h K); specific enthalpy (kJ/kg) |
| $h_0^\circ$ | enthalpy of formation (kJ/kg) |
| $I$ | irreversibility (kJ) |
| $K$ | overall thermal conductivity (kJ/m h K) |
| $k_1$ | thermal conductivity of magnesite stamp (kJ/m h K) |
| $k_2$ | thermal conductivity of chromium–magnesite brick (kJ/m h K) |
| $k_3$ | thermal conductivity of firebrick (kJ/m h K) |
| $k_4$ | thermal conductivity of steel sheet (kJ/m h K) |
| $m$ | mass (kg) |
| $M$ | molecular weight (kg) |
| $n$ | number of kmol (kmol) |
| $Pr$ | Prandtl number |
| $\dot{Q}$ | rate of heat (kcal/h) |
| $Q_{loss}$ | heat loss (kJ) |
| $r$ | radial parameter (m) |
| $s$ | specific entropy (kJ/kg K) |
| $S$ | total entropy (kJ/K) |
| $s_{298}$ | absolute entropy at standard conditions (kJ/kg K) |
| $T_1$ | inner surface temperature of furnace (K) |
| $T_5$ | outer surface temperature of furnace (K) |
| $T_S$ | temperature of surface (K) |
| $V$ | volume ($m^3$) |
| $W$ | work (kJ) |

*Greek symbols*

| | |
|---|---|
| $\varsigma$ | second law efficiency |
| $\varepsilon$ | emission coefficient |
| $\rho$ | density (kg/$m^3$) |
| $\sigma$ | Stefan–Boltzmann constant |

*Superscript*

| | |
|---|---|
| $^-$ | bar over symbol denotes property on a molar basis |
| $^\circ$ | property at standard-state condition |

*Subscript*

| | |
|---|---|
| 0 | property of surroundings |
| 1s | first surface |

| | |
|---|---|
| 2s | second surface |
| abs | absorption |
| act | actual |
| bm | bottom material |
| cond | conduction |
| conv | convection |
| cov | cover |
| elktd | electrodes |
| i | inlet |
| j | outlet |
| P | products |
| R | reactants |
| rad | radiation |
| rd | radial |
| rev | reversible |

## 2. Fundamental metallurgical principles of steel production in the electric arc furnace

The production of steel of a desired composition is realized as a result of bringing some of the elements to the desired amounts after many chemical reactions occurring at different velocities between the elements or compounds at high temperatures and adding alloy materials for the other elements needed in the composition. The basic chemical reactions taking place in the electric arc furnace (EAF) (Fig. 1) are given in Table 1 and can also be found in Refs. [3–5].

The steel production process in an electric arc furnace can be defined in the following order [3–5]:

- scrap charge,
- melting,
- oxidation,
- reduction,
- alloying,
- deoxidization,
- casting,
- preparation of furnace.

## 3. Thermodynamic analysis in the EAF

### *3.1. The first law analysis*

When the first law of thermodynamics is applied to the EAF, assuming a steady state, steady flow process and neglecting changes of the potential and kinetic energies, the actual work given to the system can be calculated as follows [6,7]:

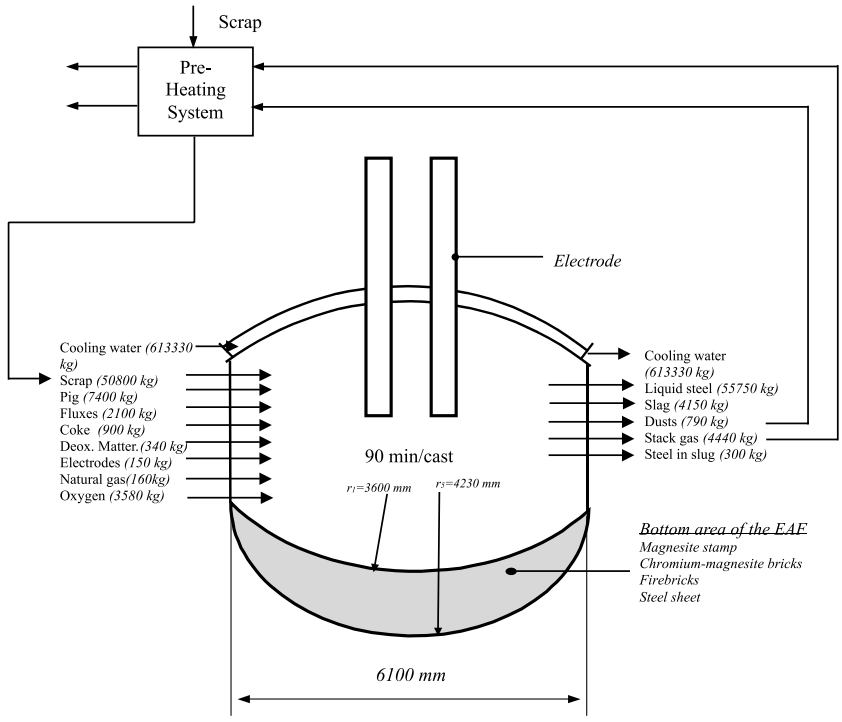


Fig. 1. EAF and mass balance.

Table 1
Standard reactions occurring in the EAF

| Reactions |
|---|
| $2[Fe] + 3[O] \rightarrow [Fe_2O_3]$ |
| $[Fe] + [O] \rightarrow [FeO]$ |
| $[C] + [O] \rightarrow CO_{(g)}$ |
| $[Si] + 2[O] \rightarrow [SiO_2]$ |
| $[Mn] + [O] \rightarrow [MnO]$ |
| $2[P] + 5[O] \rightarrow [P_2O_5]$ |
| $2[Cr] + 3[O] \rightarrow [Cr_2O_3]$ |
| $(CaO) + [S] \rightarrow (CaS) + [O]$ |
| $(CaCO_3) \rightarrow (CaO) + CO_{2(g)}$ |
| $2[Al] + 3[O] \rightarrow [Al_2O_3]$ |
| $[Ca] + [O] \rightarrow (CaO)$ |
| $[Zn] + [O] \rightarrow [ZnO]$ |
| $2[B] + 3[O] \rightarrow [B_2O_3]$ |
| $CH_{4(g)} + 2O_{2(g)} \rightarrow CO_{2(g)} + 2H_2O_{(g)}$ |
| $C_2H_{6(g)} + 7/2O_{2(g)} \rightarrow 2CO_{2(g)} + 3H_2O_{(g)}$ |
| $C_3H_{8(g)} + 5O_{2(g)} \rightarrow 3CO_{2(g)} + 4H_2O_{(g)}$ |

[ ]: solid; ( ): liquid; (g): gas.

$$W_{act} = \sum_{j} n_j[\bar{h}_0^{\circ} + \Delta\bar{h}]_j + \sum_{P} n_P[\bar{h}_0^{\circ} + \Delta\bar{h}]_P - \sum_{i} n_i[\bar{h}_0^{\circ} + \Delta\bar{h}]_i - \sum_{R} n_R[\bar{h}_0^{\circ} + \Delta\bar{h}]_R + \int dQ_{loss} \tag{1}$$

where

$$\sum_{P} n_P[\bar{h}_0^{\circ} + \Delta\bar{h}]_P = n_{Fe_2O_3}\Theta_{Fe_2O_3} + n_{FeO}\Theta_{FeO} + n_{CO}\Theta_{CO} + n_{SiO_2}\Theta_{SiO_2} + n_{MnO}\Theta_{MnO} + n_{P_2O_5}\Theta_{P_2O_5} + n_{Cr_2O_3}\Theta_{Cr_2O_3} + n_{CaS}\Theta_{CaS} + n_O\Theta_O + n_{CaO}\Theta_{CaO} + n_{CO_2}\Theta_{CO_2} + n_{Al_2O_3}\Theta_{Al_2O_3} + n_{ZnO}\Theta_{ZnO} + n_{B_2O_3}\Theta_{B_2O_3} + n_{H_2O}\Theta_{H_2O} \tag{1a}$$

$$\sum_{R} n_R[\bar{h}_0^{\circ} + \Delta\bar{h}]_R = n_{Fe}\Theta_{Fe} + n_O\Theta_O + n_C\Theta_C + n_{Si}\Theta_{Si} + n_{Mn}\Theta_{Mn} + n_P\Theta_P + n_{Cr}\Theta_{Cr} + n_{CaO}\Theta_{CaO} + n_S\Theta_S + n_{CaCO_3}\Theta_{CaCO_3} + n_{Al}\Theta_{Al} + n_{Ca}\Theta_{Ca} + n_{Zn}\Theta_{Zn} + n_B\Theta_B + n_{CH_4}\Theta_{CH_4} + n_{C_2H_6}\Theta_{C_2H_6} + n_{C_3H_8}\Theta_{C_3H_8} \tag{1b}$$

$$\Theta = [\bar{h}_0^{\circ} + \Delta\bar{h}] \tag{1c}$$

The temperature of materials going in and out of the EAF is given in Table 2.

### 3.2. The second law analysis

By applying the second law to the steady flow systems depicted in Figs. 2 and 3, we obtain the following equations, both for reversible and actual work and the other heat fluxes.

$$dW_{rev} = dW_{act} - dW' + dQ_0 \tag{2}$$

$$dW_{act} = \sum dm_j h_j + \sum dm_P h_P - \sum dm_i h_i - \sum dm_R h_R + dQ_{loss} \tag{3}$$

$$dW' = dQ_{loss} - dQ_0 = dQ_{loss}\left(1 - \frac{T_0}{T}\right) \quad \text{(from Carnot engine)} \tag{4}$$

$$dQ_{loss} = T\left[\sum dm_i s_i + \sum dm_R s_R - \sum dm_j s_j - \sum dm_P s_P\right] \quad \text{(using Fig. 3)} \tag{4a}$$

Table 2
The temperature of materials going in and out of the EAF [8]

| Material going in the EAF | Temperature (K) | Material going out the EAF | Temperature (K) |
|---|---|---|---|
| Scrap | 298–500 | Liquid steel | 1873 |
| Pig | 298 | Slag | 1873 |
| Fluxes | 298 | Dusts | 1673 |
| Coke | 298 | Stack gas | 1673 |
| Deox. Matter. | 298 | Steel in slug | 1873 |
| Electrodes | 298 | Cooling water | 311 |
| Natural gas | 298 | | |
| Cooling water | 303 | | |

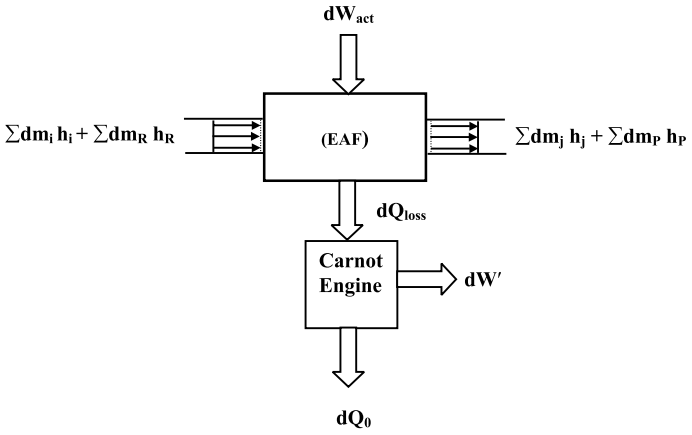


Fig. 2. Energy equilibrium of the EAF.

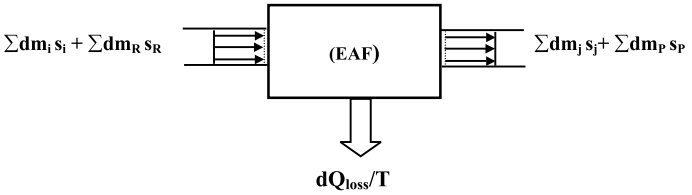


Fig. 3. The entropy equilibrium of the EAF.

$$\mathrm{d}Q_0 = \frac{T_0}{T}\mathrm{d}Q_{\mathrm{loss}} = T_0\Big[\sum \mathrm{d}m_{\mathrm{i}}s_{\mathrm{i}} + \sum \mathrm{d}m_{\mathrm{R}}s_{\mathrm{R}} - \sum \mathrm{d}m_{\mathrm{j}}s_{\mathrm{j}} - \sum \mathrm{d}m_{\mathrm{P}}s_{\mathrm{P}}\Big] \tag{5}$$

where

$\mathrm{d}W_{\mathrm{rev}}$ is the reversible work given to the EAF,
$\mathrm{d}W_{\mathrm{act}}$ is the actual work given to the EAF,
$\mathrm{d}W'$ is the work obtained from a Carnot engine,
$\mathrm{d}Q_0$ is the lost heat from a Carnot engine. This is provided from electrical energy,
$\mathrm{h} = [h_0^{\circ} + \Delta h]$, $s = [s_0^{\circ} + \Delta s]$

Eq. (6) can be obtained from Eqs. (2), (3), (4) and (5) with the related chemical reactions on a molar basis.

$$W_{\mathrm{rev}} = \sum_{\mathrm{j}} n_{\mathrm{j}}\Big[\bar{h}_0^{\circ} + \Delta\bar{h} - T_0\bar{s}\Big]_{\mathrm{j}} + \sum_{\mathrm{P}} n_{\mathrm{P}}[\bar{h}_0^{\circ} + \Delta\bar{h} - T_0\bar{s}]_{\mathrm{P}} - \sum_{\mathrm{i}} n_{\mathrm{i}}[\bar{h}_0^{\circ} + \Delta\bar{h} - T_0\bar{s}]_{\mathrm{i}}$$
$$- \sum_{\mathrm{R}} n_{\mathrm{R}}[\bar{h}_0^{\circ} + \Delta\bar{h} - T_0\bar{s}]_{\mathrm{R}} + \int_1^2 \mathrm{d}Q_{\mathrm{loss}}\left(\frac{T_0}{T}\right) \tag{6}$$

where

$$\sum_{\mathrm{P}} n_{\mathrm{P}}\left[\bar{h}_0^{\circ}+\Delta\bar{h}-T_0\bar{s}\right]_{\mathrm{P}} = n_{\mathrm{Fe_2O_3}}\Gamma_{\mathrm{Fe_2O_3}}+n_{\mathrm{FeO}}\Gamma_{\mathrm{FeO}}+n_{\mathrm{CO}}\Gamma_{\mathrm{CO}}+n_{\mathrm{SiO_2}}\Gamma_{\mathrm{SiO_2}}+n_{\mathrm{MnO}}\Gamma_{\mathrm{MnO}} + n_{\mathrm{P_2O_5}}\Gamma_{\mathrm{P_2O_5}}+n_{\mathrm{Cr_2O_3}}\Gamma_{\mathrm{Cr_2O_3}}+n_{\mathrm{CaS}}\Gamma_{\mathrm{CaS}}+n_{\mathrm{O}}\Gamma_{\mathrm{O}}+n_{\mathrm{CaO}}\Gamma_{\mathrm{CaO}} + n_{\mathrm{CO_2}}\Gamma_{\mathrm{CO_2}}+n_{\mathrm{Al_2O_3}}\Gamma_{\mathrm{Al_2O_3}}+n_{\mathrm{ZnO}}\Gamma_{\mathrm{ZnO}}+n_{\mathrm{B_2O_3}}\Gamma_{\mathrm{B_2O_3}}+n_{\mathrm{H_2O}}\Gamma_{\mathrm{H_2O}} \tag{6a}$$

$$\sum_{\mathrm{R}} n_{\mathrm{R}}\left[\bar{h}_0^{\circ}+\Delta\bar{h}-T_0\bar{s}\right]_{\mathrm{R}} = n_{\mathrm{Fe}}\Gamma_{\mathrm{Fe}}+n_{\mathrm{O}}\Gamma_{\mathrm{O}}+n_{\mathrm{C}}\Gamma_{\mathrm{C}}+n_{\mathrm{Si}}\Gamma_{\mathrm{Si}}+n_{\mathrm{Mn}}\Gamma_{\mathrm{Mn}}+n_{\mathrm{P}}\Gamma_{\mathrm{P}}+n_{\mathrm{Cr}}\Gamma_{\mathrm{Cr}} + n_{\mathrm{CaO}}\Gamma_{\mathrm{CaO}}+n_{\mathrm{S}}\Gamma_{\mathrm{S}}+n_{\mathrm{CaCO_3}}\Gamma_{\mathrm{CaCO_3}}+\mathrm{n}_{\mathrm{Al}}\Gamma_{\mathrm{Al}}+n_{\mathrm{Ca}}\Gamma_{\mathrm{Ca}} + n_{\mathrm{Zn}}\Gamma_{\mathrm{Zn}}+n_{\mathrm{B}}\Gamma_{\mathrm{B}}+n_{\mathrm{CH_4}}\Gamma_{\mathrm{CH_4}}+n_{\mathrm{C_2H_6}}\Gamma_{\mathrm{C_2H_6}}+n_{\mathrm{C_3H_8}}\Gamma_{\mathrm{C_3H_8}} \tag{6b}$$

$$\Gamma = [\bar{h}_0^{\circ}+\Delta\bar{h}-T_0\bar{s}] \tag{6c}$$

$$\Delta\bar{h} = \bar{h}_T-\bar{h}_{298} = \int_{298}^{T}\bar{c}_{\mathrm{p}}\mathrm{dT} \tag{7}$$

$$\Delta\bar{s} = \bar{s}_T-\bar{s}_{298} = \int_{298}^{T}\left(\frac{\bar{c}_{\mathrm{p}}}{T}\right)\mathrm{dT} \tag{8}$$

$$\bar{c}_{\mathrm{p}} = a+bT+cT^{-2} \tag{9}$$

$$\int_1^2 \mathrm{d}Q_{\mathrm{loss}} = \int_1^2 \mathrm{d}Q_{\mathrm{abs}}+\int_1^2 \mathrm{d}Q_{\mathrm{cond}}+\int_1^2 \mathrm{d}Q_{\mathrm{rad}}+\int_1^2 \mathrm{d}Q_{\mathrm{conv}} \tag{10}$$

The coefficients $a$, $b$ and $c$ are given in Table 3 and were found experimentally for the materials [9,10].

### 3.3. Calculation of the heat lost

#### 3.3.1. The heat absorbed at the bottom of the EAF

The bottom of the electric arc furnace is made of steel sheet. The magnesite stamp, chromium–magnesite bricks and firebricks are placed, respectively, on this steel sheet. The chemical analyses of the bottom materials are investigated, and then, according to these analyses, the $\bar{c}_{\mathrm{p}}$ functions of these materials are formed. In order to calculate the heat absorbed by these materials, the mass and volume of each material it has to be known. The volume can be obtained using Eq. (11) [11] and the heat by using Eq. (12).

$$V = \int\int\int r^2\sin\theta\,\mathrm{d}r\,\mathrm{d}\theta\,\mathrm{d}\Phi = 0.4(r_2^3-r_1^3) \quad r_1\leqslant r\leqslant r_2;\quad 0\leqslant\theta\leqslant 0.2\pi;\quad 0\leqslant\Phi\leqslant 2\pi \tag{11}$$

$$Q_{\mathrm{abs}} = \left(\frac{\rho_{\mathrm{bm}}V}{M_{\mathrm{bm}}}\right)\bar{c}_{\mathrm{p}}\Delta T \tag{12}$$

Table 3
Constant pressure specific heat and coefficients $a$, $b$ and $c$ of some substances used in the EAF [9,10]

| Substance | $a$ | $b$ | $c$ | $\bar{c}_p = a + bT + cT^{-2}$ (kcal/kmol K) |
|---|---|---|---|---|
| $\langle Fe\rangle\alpha$ | 4.18 | $5.92 \times 10^{-3}$ | 0 | $4.18 + 5.92 \times 10^{-3}T$ $(273 < T < 1033)$ |
| $\langle Fe\rangle\beta$ | 9.0 | 0 | 0 | 9.0 $(1033 < T < 1181)$ |
| $\langle Fe\rangle\gamma$ | 1.84 | $4.66 \times 10^{-3}$ | 0 | $1.84 + 4.66 \times 10^{-3}T$ $(1181 < T < 1674)$ |
| $\langle Fe\rangle\delta$ | 10.5 | 0 | 0 | 10.5 $(1674 < T < \text{mp})$ |
| {Fe} | 10 | 0 | 0 | 10 $(\text{mp} < T < 1873)$ |
| C | 4.1 | $1.02 \times 10^{-3}$ | $-2.1 \times 10^{5}$ | $4.1 + 1.02 \times 10^{-3}T - 2.1 \times 10^{5}T^{-2}$ |
| $\langle Si\rangle$ | 5.72 | $0.59 \times 10^{-3}$ | $0.99 \times 10^{5}T^{-2}$ | $5.72 + 0.59 \times 10^{-3}T - 0.99 \times 10^{5}T^{-2}$ $(298 < T < \text{mp})$ |
| {Si} | 6.12 | 0 | 0 | 6.12 $(\text{mp} < T < 1873)$ |
| $\langle Mn\rangle_{\alpha}$ | 5.7 | $3.38 \times 10^{-3}$ | 0 | $5.7 + 3.38 \times 10^{-3}T$ $(298 < T < 1000)$ |
| $\langle Mn\rangle_{\beta}$ | 8.33 | $0.66 \times 10^{-3}$ | $0.37 \times 10^{5}$ | $8.33 + 0.66 \times 10^{-3}T + 0.37 \times 10^{5}T^{-2}$ $(1000 < T < 1374)$ |
| $\langle Mn\rangle_{\gamma}$ | 10.7 | 0 | $5 \times 10^{5}$ | $10.7 + 5 \times 10^{5}T^{-2}(1374 < T < 1410)$ |
| $\langle Mn\rangle_{\delta}$ | 11.3 | 0 | 0 | 11.3 $(1410 < T < \text{mp})$ |
| {Mn} | 11 | 0 | 0 | 11 $(\text{mp} < T < \text{bp})$ |

$\langle\rangle$: solid-phase; {}: liquid-phase; $\langle\rangle_{\alpha}$: $\alpha$-phase; $\langle\rangle_{\beta}$: $\beta$-phase; $\langle\rangle_{\gamma}$: $\gamma$-phase; $\langle\rangle_{\delta}$: $\delta$-phase; mp: melting point; bp: boiling point.

### 3.3.2. Heat loss caused by conduction through the bottom of the EAF

The bottom area can be obtained by using Eq. (13) [11]. The bottom heat loss due to conduction can be calculated using Eqs. (14) and (15).

$$A_{rd} = r^2 \int\int \sin\theta \, d\theta \, d\Phi = 1.2r^2; \quad 0 \leqslant \theta \leqslant 0.2\pi; \quad 0 \leqslant \Phi \leqslant 2\pi \tag{13}$$

$$\dot{Q}_{cond} = -kA_{rd}\left(\frac{dT}{dr}\right) \tag{14}$$

$$\dot{Q}_{cond} = 1.2K(T_1 - T_5) \tag{15}$$

where,

$$1/K = 1/k_1(1/r_1 - 1/r_2) + 1/k_2(1/r_2 - 1/r_3) + 1/k_3(1/r_3 - 1/r_4) + 1/k_4(1/r_4 - 1/r_5)$$

These numerical values are given in Table 4.

### 3.3.3. Heat loss from the cover of the EAF caused by radiation and convection

During production, the cover of the arc furnace is opened for scrap and other charging. When the cover is opened, heat is transferred from the surface of the liquid steel to the surroundings by means of radiation and convection. The heat loss caused by radiation and convection can be calculated from the following relations [12]:

$$\dot{Q}_{rad} = \sigma\varepsilon A_{cov}(T_s^4 - T_0^4) \tag{16}$$

Table 4
Numerical values of bottom area of the EAF

| Bottom of the EAF | $r$ (mm) | $k$ (kJ/h m K) | $T$ (K) |
|---|---|---|---|
| Magnesite stamp | $r_1 = 3600$ | $k_1 = 4.18$ | $T_1 = 1873$ |
| Chromium– | $r_2 = 3861$ | $k_2 = 7$ | $T_2 = 978$ |
| Magnesite bricks | $r_3 = 4122$ | $k_3 = 4.4$ | $T_3 = 509$ |
| Firebricks | $r_4 = 4200$ | | $T_4 = 305$ |
| Steel sheet | $r_5 = 4230$ | $k_4 = 185$ | $T_5 = 303$ |

Between $_{1–2}$: Magnesite stamp; $_{2–3}$: Chromium–magnesite bricks; $_{3–4}$: Firebricks; $_{4–5}$: Steel sheet.

$$\text{if } D/L \geqslant 35/Gr_L^{1/4} \tag{17}$$

$$Nu = c(GrPr)^m = h\left(\frac{L}{k}\right) \tag{18}$$

$$\dot{Q}_{\text{conv}} = c(GrPr)^m\left(\frac{k}{L}\right)hA_{\text{cov}}\Delta T \tag{19}$$

where $h$ is the heat transfer coefficient. The values of coefficients $c$ and $m$ are given according to multiplication of the $Gr$ and $Pr$ numbers [12].

### 3.3.4. Heat loss from electrodes

Conducting very high currents, the electrodes transmit the electric energy to the arc area (see Fig. 4 and Table 5). This causes them to absorb a certain amount of energy as a heat source. During charging into the arc furnace, heat is transferred from the electrodes that are pulled from

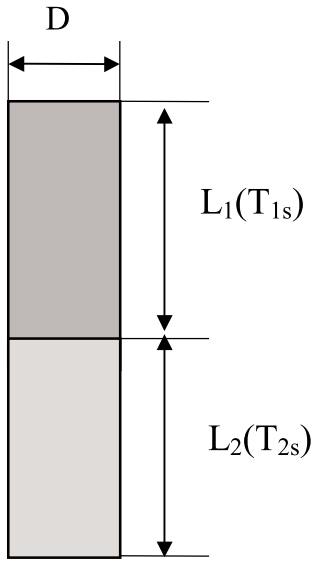


Fig. 4. Electrode.

Table 5
Properties of electrode

| $D$ (m) | $L_1$ (m) | $L_2$ (m) | $\rho$ (kg/m$^3$) | $T_{1s}$ (°C) | $T_{2s}$ (°C) |
|---|---|---|---|---|---|
| 457 | 2 | 1.7 | 1500 | 150–200 | 1800–2000 |

the furnace to the surroundings by radiation and convection. The heat losses by convection and radiation can be given in the following, similar to Eqs. (16) and (19);

$$\dot{Q}_{\text{rad}} = \sigma \varepsilon A_{\text{elktd}} (T_s^4 - T_0^4) \tag{20}$$

$$\dot{Q}_{\text{conv}} = c(GrPr)^m \left(\frac{k}{L}\right) h A_{\text{elktd}} \Delta T \tag{21}$$

*3.3.5. Irreversibility*

Lost work caused by irreversibilities can be obtained by using Eq. (22):

$$I = W_{\text{act}} - W_{\text{rev}} \tag{22}$$

This is also a measure of how one can decrease the amount of energy spent in the process.

*3.3.6. The second law efficiency*

The actual work can be evaluated by using the reversible work and second law efficiency. The second law efficiency can be defined as follows.

$$\varsigma = \frac{W_{\text{rev}}}{W_{\text{act}}} \tag{23}$$

An increase in the second law efficiency leads to an increase in the reversible work which causes a decrease in the actual work.

## 4. Discussion and conclusions

In this study, the second law analysis for steel production (Table 6) in an EAF has been performed.

The recovered energy is proportional to the scrap pre-heating temperature. When they both increase, the actual work, the reversible work and irreversibility decrease slowly (Fig. 5). On the other hand, the increase in the exergy efficiency is due to the decrease in the actual work being more than the decrease in the reversible work.

The second law efficiency of the system can be increased by using a pre-heating system. In this way, some of the heat lost with the stack gas to the surrounding can be recovered.

The amount of recovered energy from the system can be increased by applying pre-heating.

Modernization of the pre-heating system or use of newly constructed heat recovery systems is very helpful in increasing the second law efficiency [8].

Table 6
Chemical analysis of liquid steel obtained from the EAF

| Chemical compound | Amount (kg) | Percent (%) | Molar amount (kmol) |
|---|---|---|---|
| Fe | 55,116 | 98.86 | 984 |
| C | 56 | 0.1 | 4.6 |
| Si | 28 | 0.05 | 1 |
| Mn | 200 | 0.36 | 3.6 |
| P | 8 | 0.01 | 0.3 |
| S | 22 | 0.04 | 0.7 |
| Cr | 84 | 0.15 | 1.6 |
| Ni | 69 | 0.12 | 1.2 |
| Mo | 50 | 0.09 | 0.5 |
| Cu | 117 | 0.21 | 1.8 |
| Total | 55,750 | 100 | |

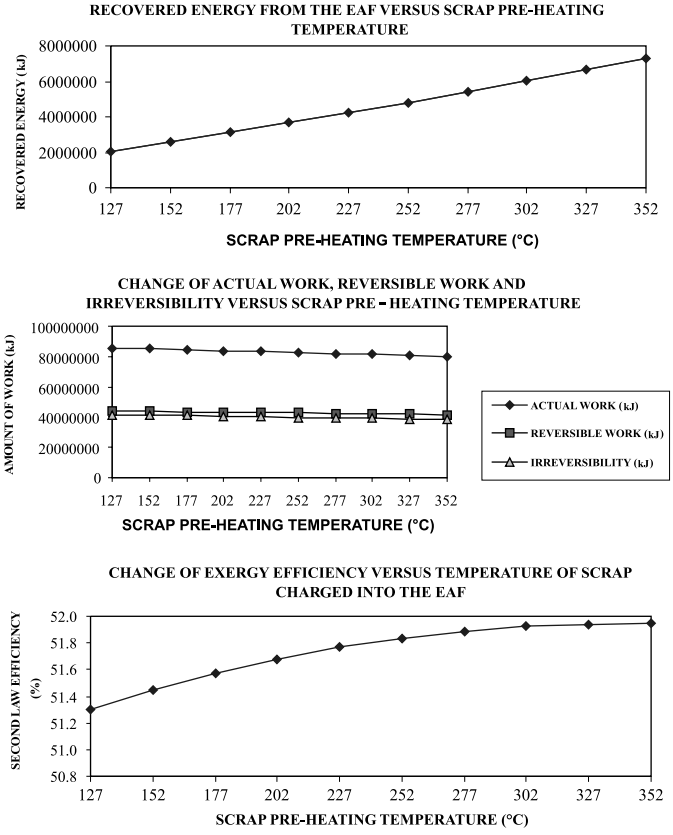


Fig. 5. Charts showing the changes of convected energy, amount of works and exergy efficiency versus the temperature of scrap charged into the EAF.

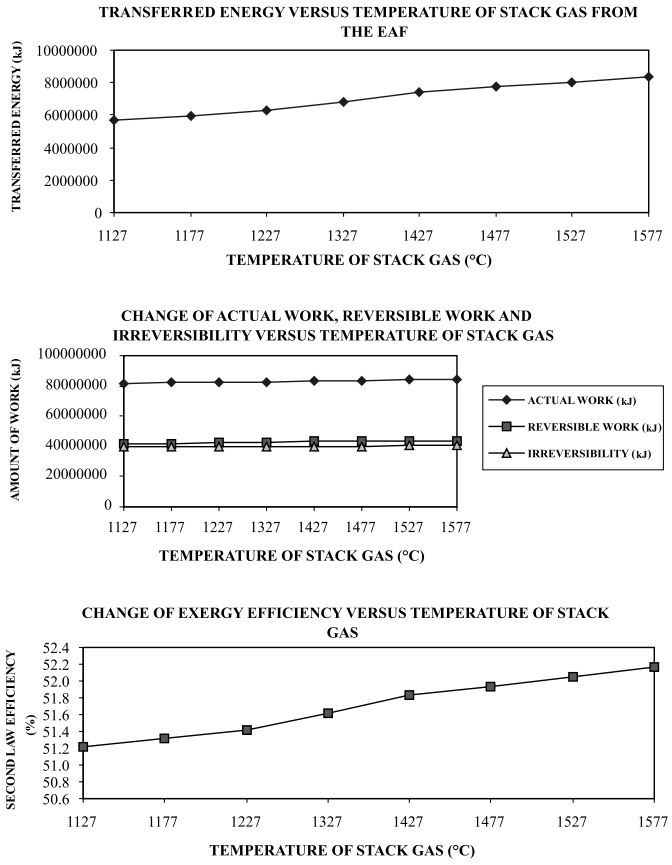


Fig. 6. Charts showing the changes of transferred energy, amount of works and exergy efficiency versus the outlet temperature of stack gas.

As the stack gas temperature increases, the transferred energy from the EAF increases. At the same time, the actual work, reversible work and irreversibility also increase slowly with the increase in stack gas temperature (Fig. 6).

The energy transferred from the stack gas and dusts can be used more effectively in a scrap pre-heating system. It is possible to use the unused portion of this energy in other applications.

As the cooling water temperature increases, the transferred energy from the EAF increases. Accordingly, the actual work, reversible work and irreversibility increase with the increase in cooling water temperature. However, the exergy efficiency decreases with the cooling water temperature because the increase in actual work is more than that in the reversible work, as shown in Fig. 7.

The heat transfer from the upper surface of the EAF is used for heating the water. In addition to being used as a primary working fluid in a steam generator or hot water producing systems, the cooling water has another function of prolonging the life of the refractors of the furnace.

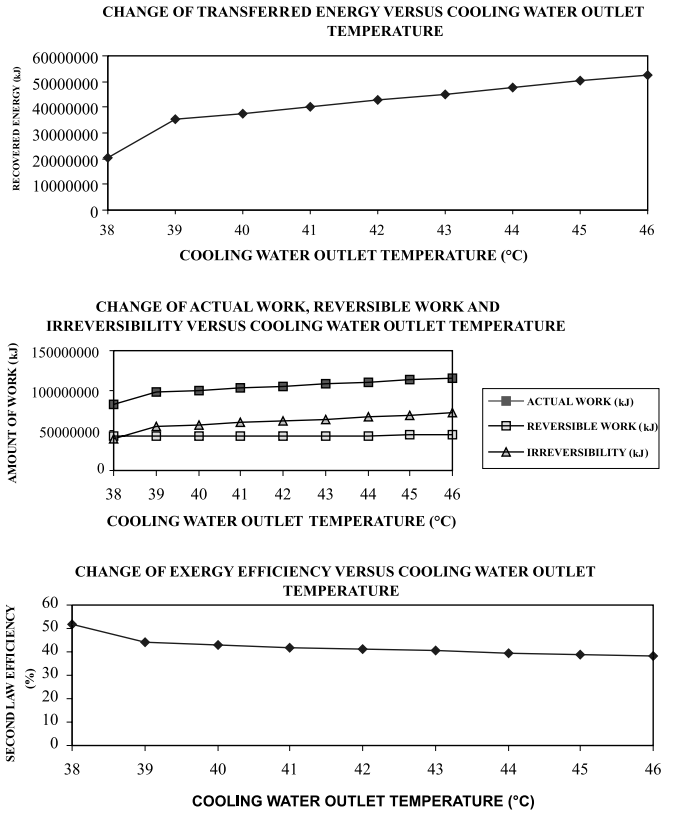


Fig. 7. Charts showing the changes of transferred energy, amount of works and exergy efficiency versus cooling water outlet temperature.

## References

[1] Bidini G, Stecco S. A computer code using exergy for optimizing thermal plants. J Eng Gas Turb Power 1991;113:145–50.
[2] Bisio G. Exergy method for efficient energy resource use in the steel industry. Energy 1993;18:971–85.
[3] Schroeder D. Use of energies in electric furnace steel making shops. New York: John Wiley & Sons Inc.; 1990.
[4] Pluckinger E, Ettering O. Electric furnace steel production. New York: John Wiley & Sons Inc.; 1979.
[5] Lankford WT, Samways NL, Craven RF, McGannon HE. The making, shaping and treating of steel. United States Steel. Tenth ed. USA; 1985.
[6] Van Wylen GJ, Sonntag RE. Fundamentals of classical thermodynamics, SI Version. New York: John Wiley & Sons Inc.; 1985.
[7] Çengel YA, Boles MA. Thermodynamics, An engineering approach. McGraw Hill Book Company; 1989.
[8] Çamdalı, Ü. The second law analysis of thermodynamics in steel production by electric arc furnace method at a steel producing company. Istanbul Technical University Institute of Science & Technology. Ph.D. Thesis, March 1998 (in Turkish).
[9] Kubaschewski O, Evans EL, Alcock CB. Metallurgical thermo-chemistry. Pergamon Press; 1989.
[10] Szargut J, Morris RD, Stewart J. Exergy analysis of thermal, chemical and metallurgical processes. Berlin: Springer-Verlag; 1988.
[11] Courant R. Differential and integral calculus. In: Interscience Publishers, vol. I & II. New York: Plenum Press; 1968.
[12] Holman JP. Heat transfer. McGraw-Hill International Book Company; 1982.